Available online at www.sciencedirect.com
SCIENCE DIRECT®
Surface and Coatings Technology 176 (2004) 157–164
SURFACE & COATINGS TECHNOLOGY
www.elsevier.com/locate/surfcoat

Electrodeposited Co–Ni–Al_2O_3 composite coatings

Gang Wu[a,*], Ning Li[a], Derui Zhou[a], Kurachi Mitsuo[b]

[a]*Department of Applied Chemistry, Harbin Institute of Technology, P.O. Box 411, Harbin 150001, PR China*
[b]*Faculty of Engineering, Kyoto University, Kyoto 606-8283, Japan*

Received 27 September 2002; accepted in revised form 14 April 2003

Abstract

Composite coatings of Co–Ni–Al_2O_3 were studied by electrolytic codeposition of Co–Ni alloys and Al_2O_3 from a sulfamate electrolyte containing Al_2O_3 particles. The influence of plating parameters on the content of the co-deposited Al_2O_3 particles in Co–Ni alloys was investigated. The maximum value of co-deposited Al_2O_3 can be achieved at a particle content of 80 g l^{-1} in bath, a current density of 3 A dm^{-2}, a pH of 4.5, and a stirring rate of 100 rpm. In the process of codeposition, cathodic polarization increases with the increase of Al_2O_3 concentration in bath and cobalt ions in electrolyte caused the reduction of polarization while nickel ions do not change the polarization behavior. Surface morphology and microstructure of Co–Ni–Al_2O_3 coatings were determined by means of scanning electron microscopy, atomic force microscopy and X-ray diffraction. It was found that the phase structure of solid solution cannot be varied by codeposition of Al_2O_3 particles in Co–Ni alloys, and it only influences the growth and orientation of crystal planes. It was shown that the presence of Al_2O_3 particles in deposit greatly improves the hardness and the wear resistance of composite coatings. However, the codeposition of Al_2O_3 increases the tensile internal stress of Co–Ni–Al_2O_3 deposit. The coefficient of thermal expansion and the thermal conductivity of Co–Ni–Al_2O_3 composite coatings are varied with the increase of Co contents and the temperature.

Keywords: Electrodeposition; Composite coating; Cobalt–Nickel alloy; Alumina

1. Introduction

Inert particles (SiC, WC, Al_2O_3, SiO_2, etc.) suspended in an electrolytic bath can be co-deposited during electrodeposition. Composite coatings produced by this technique enhance physical and mechanical properties such as wear and corrosion resistance as compared to the pure metal coatings [1,2]. These improved properties mainly derive from the presence of particles dispersed in the metallic matrix and thus depend on the content and nature of particles in the coatings. Among many methods of preparing such dispersion-hardened alloys, electrodeposition is a simple and economic method of producing composite coatings. This technique involves no high-temperature or high-pressure process. Furthermore, the concentration and spacing of the particles in deposits can be controlled precisely by this method [3].

Alloys based cobalt or nickel are widely applied in different industrial fields due to their significant resistance to wear and corrosion in high-temperatures. They are also used as protection coatings for element working in aggressive environments [4,5]. However, these coatings still suffer both severe wear and oxide scaling at elevated temperatures [6].

Recently, in order to improve the physical and mechanical properties of coatings, many kinds of composite coatings based on cobalt or nickel were developed by electrodeposition method such as Ni–SiC [7,8], Ni–ZrO_2 [9], Ni–Al_2O_3 [10–12], Ni–WC [13], Ni–PSZ [14], Co–Cr_2O_3 [15], Co–TiO_2 [16] etc. Nevertheless, few articles have reported the preparation of Co–Ni alloy matrixes containing dispersed particles. The use of Co–Ni alloy can gives exceptional advantage in term of mechanical properties (hardness, chemical inertia and good behavior in friction) [17,18] and physical properties (electrocatalytic activity [19], magnetic [20]). Especially, in the last few decades, the use of Co–Ni alloys has been extended to the production of three-dimension-

*Corresponding author. Tel.: +86-451-6413721; fax: +86-451-6221048.
E-mail address: wugangl976@hotmail.com (G. Wu).

0257-8972/04/$ - see front matter © 2003 Elsevier Science B.V. All rights reserved.
doi:10.1016/S0257-8972(03)00739-4

al, complex-shaped finished components and unique articles by the method of electroforming [21]. Al_2O_3 particle has many superior properties, such as low price, good chemical stability, high microhardness and wear resistance at high-temperature [22]. Therefore, as a second phase to strength composite materials, Al_2O_3 is one of the economic and powerful materials. Taking into account the various properties depending on both the electroplating technique and hard particle addition, the aim of this work was to co-deposit Co–Ni–Al_2O_3 composite coatings and to evaluate their properties from the view of technical and engineering application.

2. Experimental procedure

In order to obtain electrodeposited composite Co–Ni–Al_2O_3 coatings, electrolytes were prepared having the following composition: 200–300 g l^{-1} $Co(NH_2SO_3)_2 \cdot 4H_2O$, 300–350 g l^{-1} $Ni(NH_2SO_3)_2 \cdot 4H_2O$ and 20 ml l^{-1} CH_3NO, to which 20–140 g l^{-1} α-Al_2O_3 particles was added. Reagents of analytical purity and distilled water were used for preparing the solution. Using an optical microscope, the mean size of the α-Al_2O_3 particles was estimated to be 0.5 μm. The Al_2O_3 particles were pretreated with acetone and warm 5% HNO_3 to remove residual organic and impurities, then washed with distilled water and dried. In addition, an ultrasonic generator was used to minimize Al_2O_3 particles agglomeration in the suspension.

The electrodeposition experiments were conducted in a 2-l capacity PVC container with heating facilities. Rectangular 80×40 mm^2 copper plates were used as substrates for the cathodes. Separate rectangular 80×25 mm^2 cobalt (99.0%) and nickel (99.9%) anodes were used. To keep constant of metal ions concentration in electrolyte, the dissolving rate of cobalt and nickel anodes was controlled by precise adjusting the current density flowing the different anodes. The solution was stirred with a magnetically driven Teflon coated stirring bar. The codeposition parameters were current density 1–9 A dm^{-2}, stirring rate 40–160 rpm, pH 3.0–5.0 and temperature 50–60 °C. To investigate the factors affecting incorporation of Al_2O_3 particles, different parameter variations and electrolytes containing different concentration of particles and metal ions were applied. The volume fraction of Al_2O_3 particles in composite coatings (denoted by V_p) was measured by gravimetric analysis. In order to assess the influence of alumina presence on the properties of coatings, Co–Ni alloys were also obtained under the same condition from a bath without alumina. Comparative tests were conducted on Co–Ni and Co–Ni–Al_2O_3 coatings.

The polarization curves for the electrolyte with different concentration of particles and metal ions were performed using an EG&G PAR 273 Potentiostat–Galvanostat controlled by an IBM compatible PC. The scan rate was 2 mV s^{-1}.

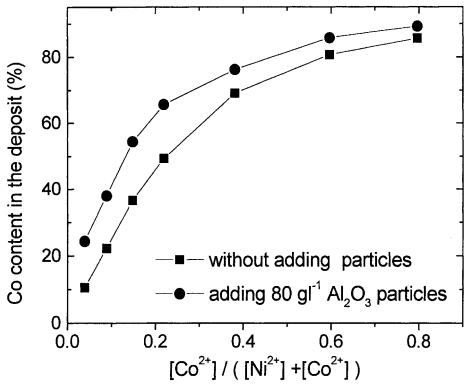

Fig. 1. Relationship between cobalt contents in solution and cobalt contents in deposit from the sulfamate electrolyte; pH 4.5, j_k=3 A dm^{-2}, T=60 °C, 100 rpm.

Surface morphology of the Co–Ni–Al_2O_3 and Co–Ni coatings was determined by scanning electron microscopy (SEM) and atomic force microscopy (AFM). The surface composition of coatings was investigated using electron dispersive spectroscopy. Phase structure of the coatings was analyzed by the X-ray diffraction (XRD).

Vickers hardness was measured by means of AKASHI Hardness tester at 100 g loads. Wear resistance was determined as weight loss per square centimeter after being exposed 20 min at the rate of 200 rpm, using a face wear test machine under a constant load of 20 kg at the temperature of 300 °C with GCrl5 abrasive wheels. The testing method of internal stress is the bent strip (cantilever beam) technique.

Coefficient of thermal expansion(CTE) was measured using NETZSCH DIL 402C Thermal Dilatometer at the temperature range 50–400 °C; Thermal conductivity was measured by the laser thermal conductivity detector at the temperature range of 150–400 °C.

3. Results and discussion

3.1. The deposition of Co–Ni–Al_2O_3 coatings

Fig. 1 shows the relationship between the Co^{2+} concentration in solution and Co contents in deposit with and without addition of Al_2O_3 particles. Whether Al_2O_3 particle was added or not, the percentage of Co in the deposit is always higher than that in the solution. This indicates the anomalous codeposition behavior of cobalt–nickel alloys was not changed by addition of Al_2O_3. Moreover, It can be seen that $A1_2O_3$ particles in electrolyte promotes the codeposition of cobalt and makes the Co contents in deposit become higher than those of without Al_2O_3 particles.

The effect of Co^{2+} concentration in electrolyte on

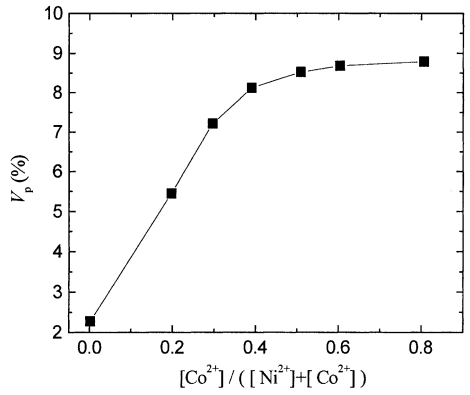

Fig. 2. The effect of concentration of Co^{2+} in solution on V_p; 80 g l^{-1} Al_2O_3, pH 4.5, j_k=3 A dm^{-2}, T=60 °C, 100 rpm.

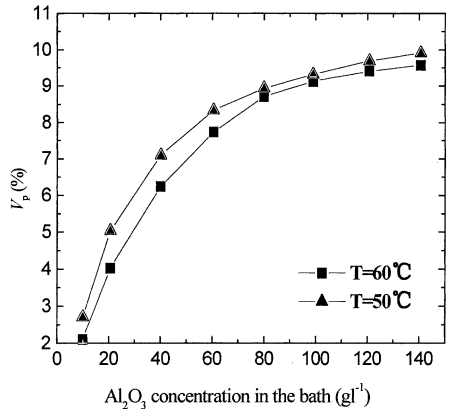

Fig. 3. Relationship between Al_2O_3 concentration in bath and V_p from electrolyte containing: 300 g l^{-1} cobalt sulfamate, 300 g l^{-1} Nickel sulfamate, j_k=3 A dm^{-2}, pH 4.5, 100 rpm.

volume percentage of Al_2O_3 particles in composite coatings V_p is shown in Fig. 2. The V_p increases with an increase of Co^{2+} concentration in bath and holds up to 0.4 ratio of $[Co^{2+}]/([Co^{2+}]+[Ni^{2+}])$, with further marginal increment at higher Co^{2+} concentration. The codeposition of Al_2O_3 is promoted by the adsorption of Co^{2+} on its surface, which increases the surface positive charge of Al_2O_3 particles.

Fig. 3 shows the relationship between concentration of Al_2O_3 particles in the electrolyte and V_p at different temperature. The ratio of $[Co^{2+}]/([Co^{2+}]+[Ni^{2+}])$ in bath is 0.5. It can be noted that Al_2O_3 in the deposit increases with an increase of Al_2O_3 in the bath, tending to attain a steady value at Al_2O_3 concentration of 80 g l^{-1}, Furthermore, as can be seen from Fig. 3, electrolyte temperature of 50 °C is more beneficial to the codeposition of Al_2O_3 than that of 60 °C, but higher temperature is useful to reduce roughness and internal stress of coatings.

Moreover, the curves are quite similar to the well-known Langmuir adsorption isotherms, supporting a mechanism based on an adsorption effect. The codeposition of Al_2O_3 by the electrodeposition technique may be attributed to the adsorption of Al_2O_3 particles on the cathode surface, as suggested by Guglielmi's two-step adsorption model [23]. Once the particle is adsorbed, metal begins building around the cathode slowly, encapsulating and incorporating the particles. The plateau observed at higher particles concentration in bath may be a result of saturation in adsorption on cathode surface.

Fig. 4 shows the effect of current density on the V_p from a bath containing 80 g l^{-1} of Al_2O_3 particles and 0.5 ratio of $[Co^{2+}]/([Co^{2+}]+[Ni^{2+}])$. It is observed that the V_p increases initially with the current density and reaches a maximum at 3.0 A dm^{-2}. Beyond this current density, the co-deposited Al_2O_3 content decreases. The maximum observed in the curve of current density vs. V_p can be attributed to the transition from an activation-controlled metal deposition reaction to a diffusion-controlled of particles transfer. The energy required to deposit for metal ion that solvated and adsorbed on the particle surface is larger than that for the freely solvated metal ions [24]. Because of the difference in activation energy needed for deposition, the initial low codeposition may be a result of the preferred free metal ions deposition. As the current density increases, this energy difference criterion becomes less important, therefore, codeposition of Al_2O_3 increases. However, at higher current densities, the loose adsorption of particles at the cathode surface may become rate controlling. Because this is always slower than the metal deposition rate, incorporation decreases with increase in current density.

The pH value of the electrolyte plays an important role in the codeposition process. The effect of pH on the V_p is shown in Fig. 5. As can be seen, the V_p attains the greatest value at pH 4.5.

To promote incorporation of the Al_2O_3 particles in deposit, the adsorption of metal ions on particle surface

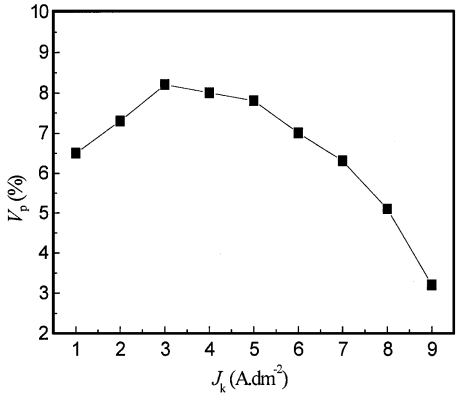

Fig. 4. The effect of current density on V_p, from electrolyte containing: 300 g l^{-1} cobalt sulfamate, 300 g l^{-1} nickel sulfamate and 80 g l^{-1} Al_2O_3, pH 4.5, T=60 °C, 100 rpm.

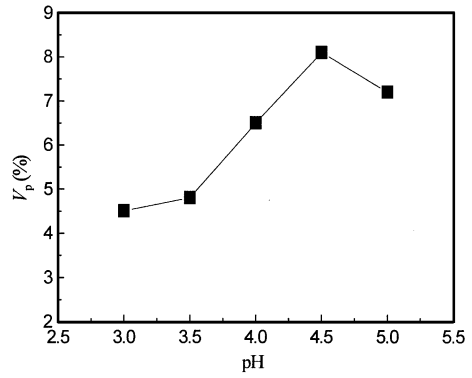

Fig. 5. Effect of the pH value on the V_p; from electrolyte containing: 300 g l^{-1} cobalt sulfamate, 300 g l^{-1} nickel sulfamate and 80 g l^{-1} Al_2O_3, j_k=3 Adm^{-2}, T=60 °C, 100 rpm.

is more useful than that of hydrogen ions [25]. The decrease of H^+ ions concentration in electrolyte contributes to the metal ions adsorption on the surface of the Al_2O_3 particles, which led to an increase in codeposition of Al_2O_3 with Co–Ni alloys.

Since Al_2O_3 particles should be transported to the cathode surface for the codeposition, the stirring rate strongly affects the content of Al_2O_3 in deposit. The influence of stirring rate on V_p is shown in Fig. 6. The V_p increases with stirring rate and reaches a maximum value at 100 rpm, then decreases with the stirring rate. The codeposition behavior of Al_2O_3 particles with Co–Ni alloys is apparently controlled by particle transfer when the stirring rate is smaller than 100 rpm. Collision factor may be the most important reason that causes codeposition of Al_2O_3 particle decrease at very rapid stirring rate [26]. Another possible reason is perhaps that the increasing streaming velocity of the suspension may also dislodge and sweep away the loosely adsorbed Al_2O_3 particles on the cathode surface, causing a reduction in codeposition.

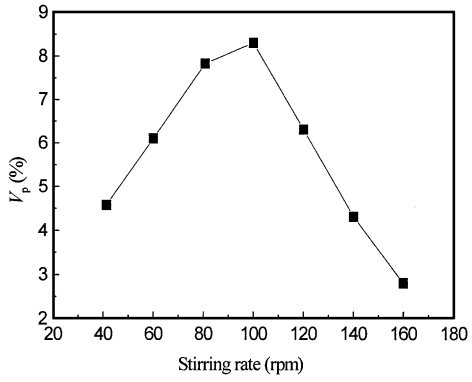

Fig. 6. Effect of the stirring rate on the V_p from electrolyte containing: 300 g l^{-1} cobalt sulfamate, 300 g l^{-1} nickel sulfamate and 80 g l^{-1} Al_2O_3, j_k=3 A dm^{-2}, T=60 °C, pH 4.5.

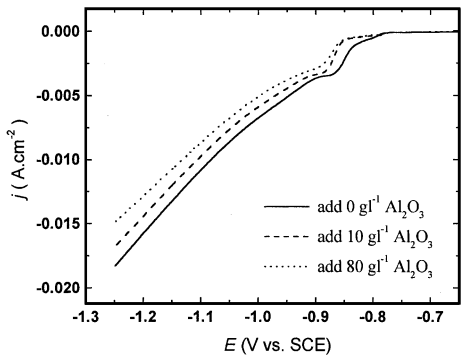

Fig. 7. Cathodic polarization curves for codeposition of Al_2O_3/Co–Ni from sulfamate electrolyte containing 300 g l^{-1} cobalt sulfamate, 300 g l^{-1} nickel sulfamate and different concentration of Al_2O_3 particles.

3.2. The polarization behavior of Co–Ni/Al_2O_3 electrolyte

The cathodic polarization behavior of the Co–Ni/Al_2O_3 electrolyte containing different concentration of Al_2O_3 particles is shown in Fig. 7. The curves represent two consecutive reduction reactions, in which H^+ and Co^{2+}/Ni^{2+} are reduced to H_2 and Co–Ni alloy, respectively. The reduction of H^+ would occur more quickly than the reduction of Co^{2+} or Ni^{2+} with the reduction potential increasing. Hydrogen evolution results in the decrease in current efficiency and has a detrimental effect on codeposition of Al_2O_3. Fig. 7 also indicates that the Al_2O_3 particles in the electrolyte cause an increase in the cathodic polarization, but the slope is unchanged. This means that the adsorption of Al_2O_3 particles on cathode surface hinders the deposition of Co^{2+} and Ni^{2+}, but does not significantly affect the electrochemical reaction mechanism.

Fig. 8 shows the cathodic polarization behavior of the electrolyte containing different Co^{2+} and constant Ni^{2+} and Al_2O_3 concentration. When the potential is

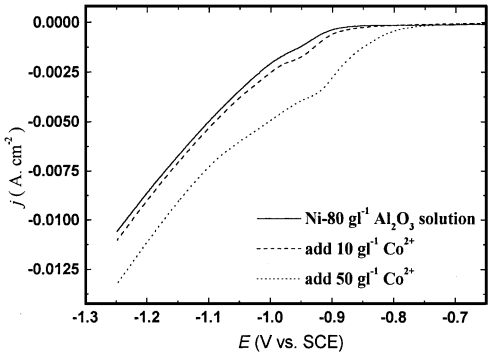

Fig. 8. Cathodic polarization curves for codeposition of Al_2O_3/Co–Ni in sulfamate electrolyte containing 300 g l^{-1} nickel sulfamate, 80 g l^{-1} Al_2O_3 and different concentration of cobalt.

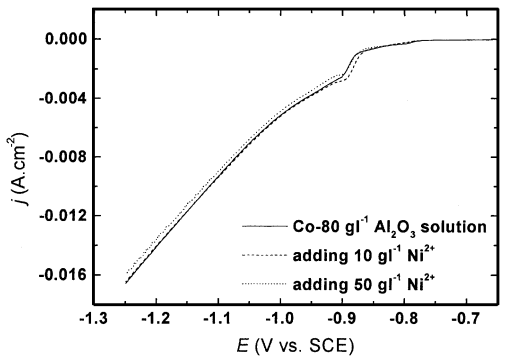

Fig. 9. Cathodic polarization curves for codeposition of Al_2O_3/Co–Ni in sulfamate electrolyte containing 300 g l^{-1} cobalt sulfamate, 80 g l^{-1} Al_2O_3 and different concentration of nickel.

polarized from -0.75 to -1.25 V vs. SCE, the increase of cobalt concentration led to an increase in the cathodic current. However, from the Fig. 9, when different Ni concentration was added in the electrolyte containing constant Co^{2+} and Al_2O_3 concentration, the cathodic polarization behavior of Co–Ni/Al_2O_3 electrolyte is almost unchanged. This phenomenon shows that the adsorption of Ni^{2+} on Al_2O_3 surface is weaker than that of Co^{2+} and cannot influence the codeposition process.

3.3. Surface morphology and microstructure

Fig. 10 compares the SEM morphology of Co–Ni coatings and Co–Ni–Al_2O_3 composite coatings. It is evident that Al_2O_3 particles are uniformly distributed in the Co–Ni matrix by electrolytic codeposition. It can be seen that the Co–Ni deposit has a rather regular surface, whereas the Co–Ni–Al_2O_3 composite coating develops a nodular surface structure. A smaller Co–Ni grain size is observed in the composite coatings compared to the Co–Ni deposits. Due to the adsorption of Al_2O_3 on the cathode surface, it increases cathodic polarization and contributes to developing fine grains. As the Co contents in the Co–Ni and Co–Ni–Al_2O_3 coatings increase from 16 to 42%, there is a decrease in grain size and the morphology changes from a nodular aspect which is related to low Co content coating to a fibril one, associated with medium Co content. Simultaneously, the surface structure became less compact. However, with the further increase of Co content ($>78\%$), more compact and fine granular morphology is observed in the Co–Ni and Co–Ni–Al_2O_3 coatings.

In order to investigate the microstructure of Co–Ni–Al_2O_3 composite coating more detailed, scanning analysis and measurements were conducted using AFM method. The results are shown in Fig. 11, Spherical growth is clearly visible on the surfaces of the composite coatings. The microstructure of Co–Ni–Al_2O_3 appears to be influenced by variations in Co contents in the composite coating. The microstructure of Ni-80Co-8.7 vol.% Al_2O_3 coating has a more uniform and fine structure than that of Ni-20Co-8.5 vol.% Al_2O_3.

The phase composition and structure of Co–Ni alloys and Co–Ni–Al_2O_3 coatings with different cobalt contents was investigated using XRD. As can be seen from Fig. 12, the crystal structures both Co–Ni coatings and

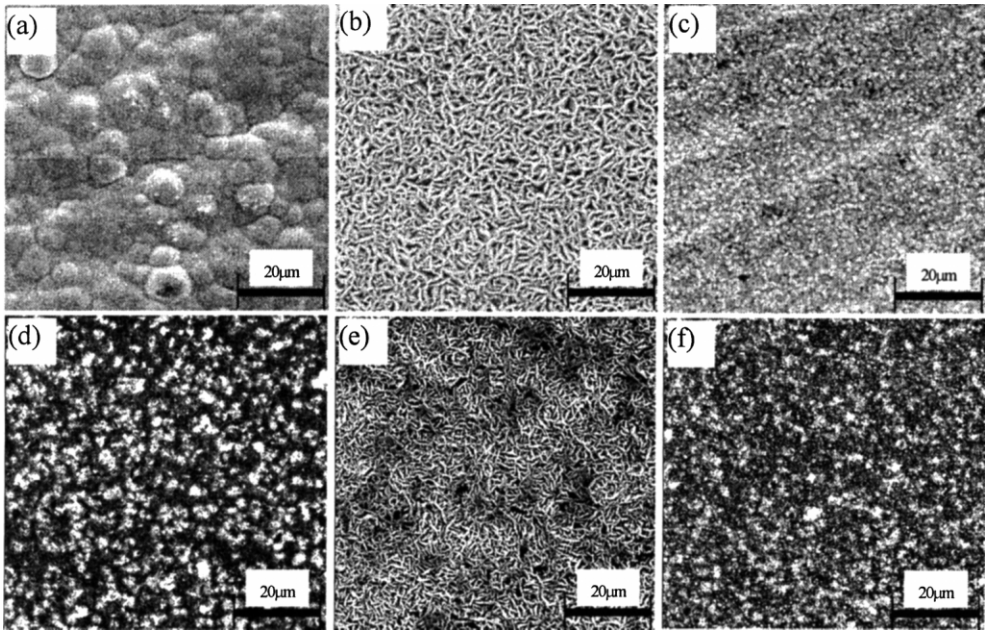

Fig. 10. SEM micrographs of Co–Ni and Co–Ni–Al_2O_3 coatings.(a) Ni-16Co; (b) Ni-40Co; (c) Ni-78Co; (d) Ni-20Co-8.5 vol.% Al_2O_3; (e) Ni-42Co-8.7 vol.% Al_2O_3; (f) Ni-80Co-8.7 vol.% Al_2O_3.

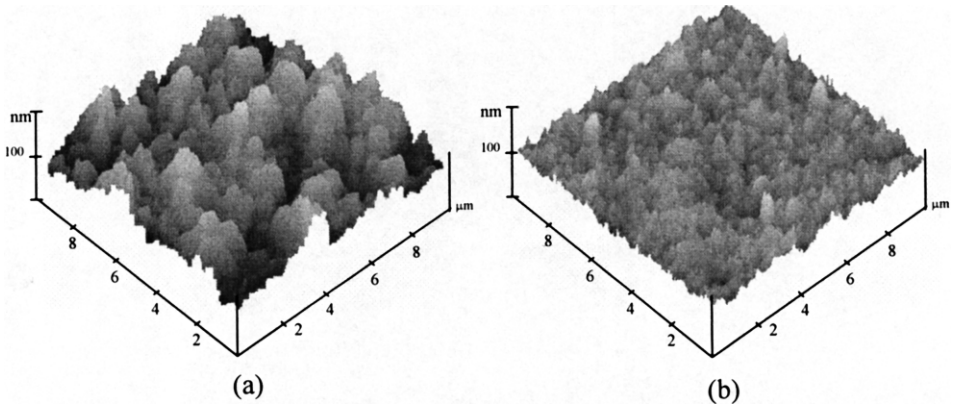

Fig. 11. AFM analysis results of Co–Ni–Al_2O_3 composite coatings.(a) Ni-20Co-8.5 vol.% Al_2O_3; (b) Ni-80Co-8.7 vol.% Al_2O_3.

Co–Ni–Al_2O_3 composite coatings are mainly dependent on the cobalt contents in deposits. For the low-cobalt coatings of Co–Ni and Co–Ni–Al_2O_3, it is confirmed the structure is single-phase solid solution of cobalt in nickel with a face-centered cubic (fcc) lattice. Nevertheless, for high-cobalt coatings of Co–Ni and Co–Ni–Al_2O_3, a solid solution of nickel in cobalt with a hexagonal close packed (hcp) lattice is obtained. The Co–Ni and Co–Ni–Al_2O_3 coatings with the low Co content all exhibit fcc nickel (1 1 1) growth orientation with significant (2 0 0), (2 2 0) and (3 1 1) reflections as well. However, at high Co content, the Co–Ni coatings show very strong hcp cobalt (2 0 0) growth orientation, while Co–Ni–Al_2O_3 composite coatings form strong hcp cobalt (1 0 0) texture. Therefore, It can be concluded that the phase structure of Co–Ni alloys solid solution is not changed by the codeposition of Al_2O_3 particles, but it obviously influences the growth and orientation of crystal planes in composite coatings, especially at high Co content.

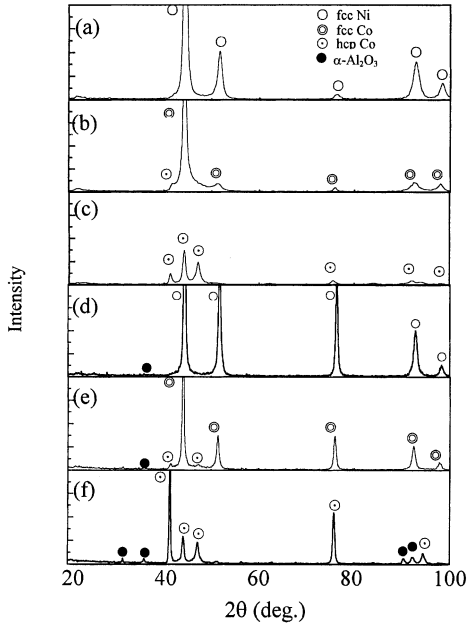

Fig. 12. XRD pattern of Co–Ni–Al_2O_3 composite coatings. (a) Ni-16Co; (b) Ni-40Co; (c) Ni-78Co; (d) Ni-20Co-8.5 vol.% Al_2O_3; (e) Ni-42Co-8.7 vol.% Al_2O_3; (f) Ni-80Co-8.7 vol.% Al_2O_3.

3.4. Mechanical properties of Co–Ni–Al_2O_3 coatings

Microhardness of the composite coatings as a function of V_p is shown in Fig. 13. As can be seen from Fig. 13, the hardness of the composite coating increases with the increase of V_p to a certain value at 5.2%, after which the increase is marginal. The improvement in the hardness of composites coating is related to the dispersion hardening effect caused by Al_2O_3 particles in the composite, which obstructs the shift of dislocation in cobalt–nickel alloys. Moreover, after annealing at 600 °C for 1 h, the microhardness of the Co–Ni–Al_2O_3 composite coatings decreases. However, when V_p in the deposit is increased from 5.2 to 8.7%, the effect of annealing on hardness is slight and the hardness remains above 520 Hv. The likely explanation to the reduction of hardness

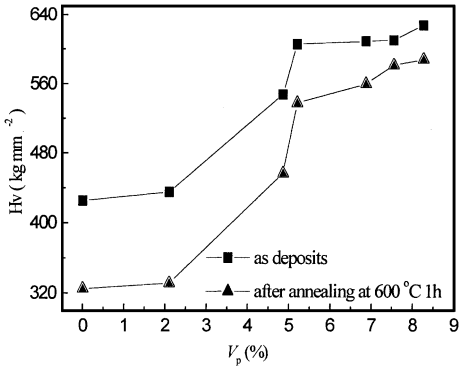

Fig. 13. The effect of V_p on Vickers Hardness of Co–Ni–Al_2O_3 composite coatings with same cobalt content.

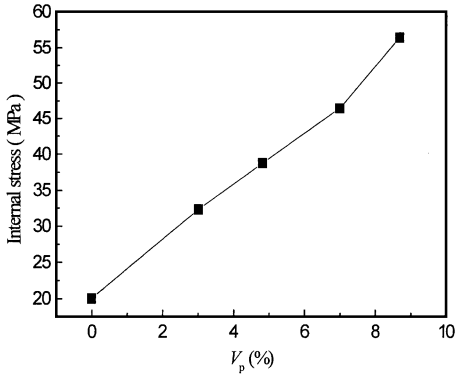

Fig. 14. The effect of V_p on internal stress of Co–Ni–Al_2O_3 composite coatings with same cobalt content.

is the recrystallization of Co–Ni alloy and the decomposition of metal hydride during annealing. The latter occurs at temperatures above 200 °C by releasing hydrogen [27].

Fig. 14 shows the effect of the V_p on the tensile internal stress of Co–Ni–Al_2O_3 composite coatings. It is shown that an increasing stress from 20 to 57 MPa is a result of increasing V_p from 0 to 8.7%. The increasing trend of internal stress is caused by the adsorption of Al_2O_3 particles on cathode surface, which makes the current efficiency decrease and the large amount of H occluded in the deposit increase. Subsequently, the desorption of H atoms causes tensile internal stress increase [28].

Wear weight loss and hardness of different coatings, including (1) Pure Nickel; (2) Pure Cobalt; (3) Ni-16Co alloy; (4) Ni-78Co alloy; (5) Ni-20Co-8.5 vol.% Al_2O_3; (6) Ni-80Co-8.7 vol.% Al_2O_3 are shown in Fig. 15. The Ni-80Co-8.7 vol.% Al_2O_3 coating has a minimum wear weight loss and maximum hardness. This result reflects that the coating with maximum hardness has the best wear resistance at high-temperature. Accord-

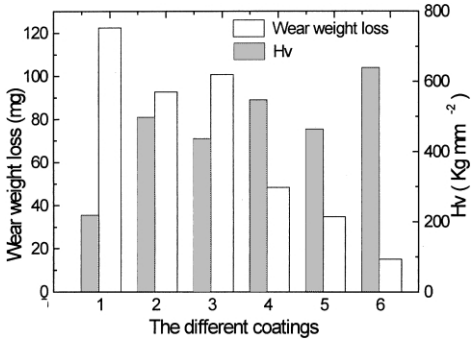

Fig. 15. The wear weight loss at 300°C and hardness of different coatings obtained by electrodeposition. (1) pure Nickel; (2) pure Cobalt; (3) Ni-16Co alloy; (4) Ni-78Co alloy;(5) Ni-20Co-8.5 vol.% Al_2O_3; (6) Ni-80Co-8.7 vol.% Al_2O_3.

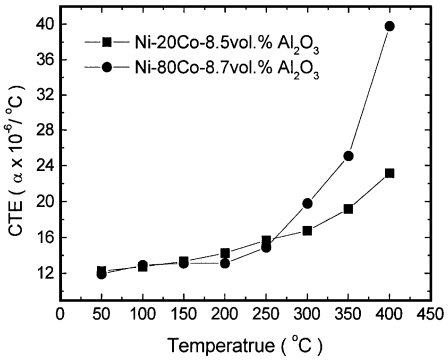

Fig. 16. The CTE of the Co–Ni–Al_2O_3 composite coatings.

ing to the data, the dispersion of Al_2O_3 particles in Co–Ni alloys enhances the surface hardness and wear resistance. Furthermore, wear resistance and hardness are dependent on the Co content. The high Co content in composite coatings contributes to improving the wear resistance and hardness of composite coatings.

3.5. Thermal physical properties of Co–Ni–Al_2O_3 coatings

When materials are to be employed at elevated temperature, knowledge of their thermal physical properties is important. Both CTE and thermal conductivity are important thermal physical properties. When a construction during application is exposed to temperature changes, the mismatch of CTE between the thin films and the substrate may lead to residual stresses and produce additional problems [29]. The higher the thermal conductivity, the more efficient the cooling property. High thermal conductivity also assures a uniform temperature distribution, which reduces thermally induced stresses, and thereby improves fatigue properties [30].

Relationship between the temperature and the CTE and thermal conductivity of Co–Ni–Al_2O_3 composite coatings are shown in Figs. 16 and 17. When tempera-

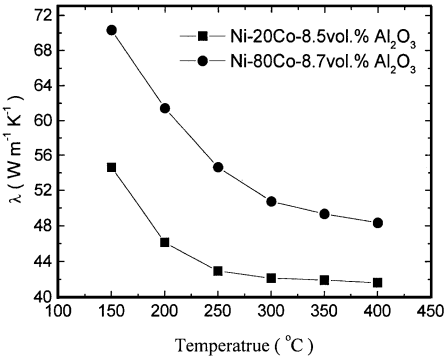

Fig. 17. Thermal conductivity of the Co–Ni–Al_2O_3 composite coatings.

ture is lower than 250 °C, CTE of two types of composite coatings are almost equal. But as the temperature above the 250 °C, CTE of Ni-80Co-8.7 vol.% Al_2O_3 coating is higher than that of Ni-20Co-8.5 vol.% Al_2O_3 coating. Fig. 17 shows the effects of temperature and cobalt content of Co–Ni–Al_2O_3 coatings on the thermal conductivity. The experimental results indicate that there is a tendency for the thermal conductivity to decrease with increasing temperature from 150 to 400 °C. The thermal conductivity of Ni-20Co-8.5 vol.% Al_2O_3 is lower than that of Ni-80Co-8.7 vol.% Al_2O_3 at the same temperature. The reason maybe is that the Ni-20Co-8.5 vol.% Al_2O_3 coating has high degree of porosity and intergranular cracking, as shown in Fig. 11 by AFM analysis. These microstructure flaws impede the flow of heat current in the composite coatings, reducing the conductivity. Furthermore, due to an increase of cobalt content in coatings, the number of scattering sites of conduction electrons increases and it improve the thermal conductivity of Co–Ni–Al_2O_3 composite coatings.

4. Conclusions

Co–Ni–Al_2O_3 composite coatings were studied by electrolytic codeposition of Co–Ni alloys and Al_2O_3 from a sulfamate electrolyte and the following conclusions can be obtained.

(1) Al_2O_3 (vol.%) in Co–Ni alloys was attained maximum value at a particle content of 80 g l^{-1}, a current density of 3 A dm^{-2}, a pH of 4.5, and a stirring rate of 100 rpm.

(2) The anomalous codeposition of cobalt–nickel alloys cannot be changed by addition of Al_2O_3 in electrolyte. However, the addition of Al_2O_3 particles in electrolyte promotes the deposition of Co in the deposit. The presence of Co^{2+} in the electrolyte also increases the codeposition amount of Al_2O_3 particles. The cathodic polarization of Co–Ni/Al_2O_3 electrolyte increases with the increase of Al_2O_3 concentration in bath. Cobalt ions in the electrolyte leads to the decrease of cathodic polarization while nickel ions do not change the polarization behavior.

(3) Surface morphology and microstructure of Co–Ni–Al_2O_3 coatings are mainly influenced by the cobalt contents. In the high-cobalt region, the coatings with hcp lattice structure have a more uniform and fine surface structure than those of the low-cobalt coatings with fcc lattice structure. The phase structure of solid solution cannot be varied by codeposition of Al_2O_3 particles in Co–Ni alloys, and it only influences the growth and orientation of crystal planes.

(4) The codeposition of Al_2O_3 particles in the deposit greatly improves the hardness and the wear resistance of composite coatings. However, it also increases the tensile internal stress of Co–Ni–Al_2O_3 coatings. The CTE and the thermal conductivity of Co–Ni–Al_2O_3 composite coatings are varied with the increase of Co contents and the temperature.

Acknowledgments

The authors would like to thank Shanghai BaoShan Iron & Steel Company for the financial support.

References

[1] B.Q. Wang, K. Luer, Wear 174 (1994) 177.
[2] A. Hovestad, L.J.J. Jansen, J. Appl. Electrochem. 25 (1995) 519.
[3] M. Musiani, Electrochim. Acta 45 (2000) 3397.
[4] D. Golodnitsky, Yu. Rosenberg, A. Ulus, Electrochim. Acta 47 (2002) 2707.
[5] L. Burzynska, E. Rudnik, Hydrometallurgy 54 (2000) 133.
[6] A.N. Correia, S.A.S. Machado, Electrochem. Acta 45 (2000) 1733.
[7] O. Berkh, A. Bodnevas, J. Zahavi, Plat. Surf. Finish. 82 (11) (1995) 62.
[8] K.K. Sun, J.Y. Hong, Surf. Coat. Technol. 108 (1998) 564.
[9] S. Balathandn, S.K. Sechadri, Met. Finish. 92 (2) (1994) 49.
[10] A. Bvidrine, E.J. Podlaha, J. Appl. Electrochem. 34 (2001) 461.
[11] B.F. Levin, J.N. Dupont, A.R. Marder, Wear 238 (2000) 160.
[12] M. Verelst, J.P. Bonino, M. Brieu, A. Rousset, Mater. Sci. Eng. A 191 (1995) 165.
[13] M. Pushpavanam, S.R. Natarajan, K. Balskrishnan, Plat. Surf. Finish. 84 (6) (1997) 88.
[14] J. Li, C.C. Dai, D.L. Wang, X.G. Hu, Surf. Coat. Technol. 91 (1997) 131.
[15] M. Thoma, Plat. Surf. Finish. 71 (9) (1984) 51.
[16] E.P. Rajiv, S.K. Seshadri, Plat. Surf. Finish. 80 (10) (1993) 66.
[17] E. Gomez, J. Ramirez, E. VaIles, J. Appl. Electrochem. 28 (1998) 71.
[18] L. Burzynska, E. Rudnik, Hydrometallurgy 54 (2000) 133.
[19] C. Fan, D.L. Piron, Surf. Coat. Technol. 73 (1995) 91.
[20] S. Armyanov, Electrochem. Acta 45 (2000) 3323.
[21] H. Tony, W. Alec, Met. Finish. 98 (2000) 388.
[22] C.C. Anya, Ceram. Int. 24 (1998) 533.
[23] N. Guglielmi, J. Electrochem. Soc. 144 (1997) 62.
[24] L. Benea, P.L. Bonora, A. Borello, J. Electrochem. Soc. 148 (2001) C461.
[25] B. Szczygiel, Plat. Surf. Finish. 84 (2) (1997) 62.
[26] S.H. Yeh, C.C. Wan, Plat. Surf. Finish. 84 (1997) 54.
[27] S. Armyanov, Svitkova, O. Blajiev, J. Appl. Electrochem. 27 (1997) 185.
[28] S. Armyanov, G. Sotirova-Chakarova, J. Electrochem. Soc. 139 (1992) 3454.
[29] A. Rudajevova, F. von Buch, J. Alloy Compd. 292 (1999) 27.
[30] V. Pal, M. Singh, B.R.K. Gupta, J. Phys. Chem. Solids 60 (1999) 1895.